Compatibility of Kraft Lignin and Phenol-Organosolv Lignin with PLA in 3D Printing and Assessment of Mechanical Recycling

ACS APPLIED POLYMER MATERIALS

pubs.acs.org/acsapm
Article

Compatibility of Kraft Lignin and Phenol-Organosolv Lignin with PLA in 3D Printing and Assessment of Mechanical Recycling

Serena Frasca, Christos S. Katsiotis, Åke Henrik-Klemens, Anette Larsson, Maria Strømme, Jonas Lindh, Maxim V. Galkin,* and Johan Gising*

Cite This: ACS Appl. Polym. Mater. 2024, 6, 13574−13584
Read Online

ABSTRACT: Lignin is an aromatic biomacromolecule with many promising properties that can be beneficial to polymer blends. The main objective of this work was to investigate the processability, compatibility, and recyclability of lignin blends with poly(lactic acid). Two different commercial kraft lignins and a phenolated organosolv lignin were blended with poly(lactic acid) at various weight percentages, targeting high lignin content (30, 50, and 70 wt %). Obtained blends were used in additive manufacturing via fused deposition modeling. All obtained materials were thoroughly characterized by tensile tests, thermogravimetric analysis, differential scanning calorimetry, and ^{31}P NMR. The recyclability of the polymer blend materials was evaluated by re-extruding them up to four times, and their printability was also assessed. The results showed that the material retained its mechanical properties relatively well for up to three cycles after which its tensile strength decreased by 30%. Phenolated organosolv lignin exhibited better printability across a broader range of lignin content compared to kraft lignin analogs while maintaining similar thermal and mechanical properties.

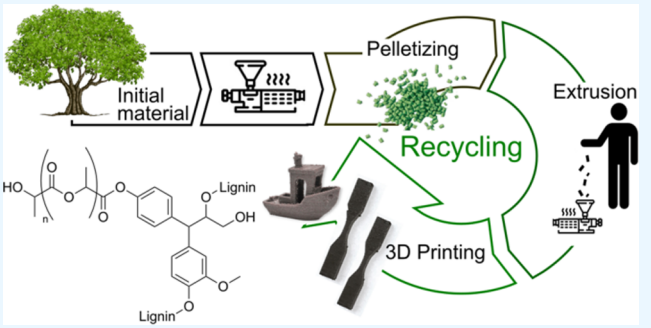

KEYWORDS: *biobased materials, recycling, poly(lactic acid), lignin, blends*

INTRODUCTION

Additive manufacturing (AM) emerged several decades ago and holds great potential for the customized, distributed, and on-demand production of parts. While various materials, including ceramics and metals, are available for three-dimensional (3D) printing, polymeric materials are most commonly used in fused deposition modeling (FDM). With increasing concerns about sustainability and the growing volume of plastic waste worldwide, the focus in AM has shifted toward eco-friendly materials. The popularity of sustainable biobased materials is increasing in 3D printing as replacements for petroleum-based thermoplastic filaments.[1] Poly(lactic acid) (PLA) is a compostable biobased alternative to fossil-based plastics.[2] Lactic acid, the precursor to PLA, can be produced from agricultural sources such as corn, and sugar cane or second-generation feedstock such as bagasse.[3] In FDM, PLA is commonly used due to its biobased nature, lower melting temperature compared to other polymers, and higher safety profile.[4] However, PLA has low thermal stability, is brittle, and suffers from a high degradation rate during processing.[5] Fillers and plasticizers can be added to mitigate drawbacks and provide new properties to the final material. Among the various proposed additives, lignin, a natural macromolecule and byproduct of pulp and paper, and ethanol production industries, is emerging as a promising option. For instance, the addition of lignin can impart new properties to PLA-based filaments while preserving their biobased nature and potential compostability.[6]

Lignin is a natural macromolecule that is a crucial component of the cell walls of primarily terrestrial plants. It is formed through the radical coupling of propylphenols, yielding structures with variable dispersity and no extended sequences of regularly repeating units. Lignin possesses several properties that make it a useful additive in polymeric materials. It exhibits high thermal stability, flame retardant,[7] UV blocking properties,[8,9] antioxidant,[10,11] and antibacterial activity.[12] By variation of the amount of lignin, it is possible to affect the hydrophobicity, stiffness, and crystallinity of PLA, thereby further adjusting its thermochemical properties. Moreover, the addition of lignin can impart a wood-like texture to filaments, enabling the creation of 3D-printed objects with a wood-like appearance and feel.[13] This makes lignin not only a functional

Received: July 16, 2024
Revised: October 21, 2024
Accepted: October 22, 2024
Published: October 31, 2024

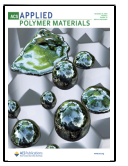

additive but also an aesthetic one, broadening the range of applications for PLA-lignin blends in AM.

There are two distinct approaches for mixing lignin with PLA (a selection of literature available on the topic is summarized and tabulated in the Supporting Information, SI). The first approach uses lignin directly, while the second involves lignin modification. Following this, lignin can be mixed with PLA either through melt blending or codissolution before being fed into an extruder. Finally, the material is extruded into filaments or pellets, which can be used directly in 3D printing. The lignin content in PLA blends typically ranges from 1 to 40 wt %.[8,12,14−18] Lower concentrations (up to 10 wt %) are used to enhance mechanical properties such as impact strength and elongation at break, while higher amounts (20−40 wt %) are explored for applications requiring enhanced thermal stability. However, higher lignin loading typically compromises the mechanical properties of the material compared with pure PLA. This observation is attributed to the lignin dispersity within the PLA matrix and the compatibility between lignin and PLA.

To address the issue of poor interfacial adhesion between PLA and lignin, several modifications to lignin have been proposed. The most common modification is acetylation, which involves treating isolated lignin with acetic anhydride in the presence of pyridine.[8,11] Acetylation reduces lignin's hydrophilicity and improves its dispersion in the PLA matrix, thereby making the components of the blend more similar in their hydrophobicity and hydrophilicity. This, in turn, is expected to yield a more thermally and mechanically stable material. To compare the material compatibility, the Hildebrand solubility parameters can be used. It was predicted that the Hildebrandt solubility parameters of acetylated lignin (20 $MPa^{0.5}$) are closer to those of PLA (20−21 $MPa^{0.5}$) compared to organosolv lignin (25 $MPa^{0.5}$) (see SI, Table S2). Consequently, acetylated lignin blends exhibit better mechanical properties and thermal stability compared with unmodified lignin blends. Other methods to improve interfacial bonding with PLA include direct PLA grafting,[9,19,20] oxypropylation,[21] silane treatment [e.g., (3-aminopropyl)triethoxysilane],[21] treatment with caprolactam,[14] and maleic anhydride and its derivatives.[22] In all cases, such treatments improve the tensile strength and reduce the brittleness of the blends. Besides modification of lignin in a separate step, in situ compatibilization with PLA can be performed during the extrusion process. However, additional treatment and postmodification of lignin can be detrimental to the overall sustainability of the material and, if possible, should be omitted. For example, reactive processing has been demonstrated for lignin under ring-opening polymerization conditions with lactide,[23] and esterification or transesterification with PLA under reactive extrusion.[17,24]

Another important aspect of material sustainability is the end-of-life of the material, including the possibility of recycling. The sustainability of PLA also relies on its degradability under industrial composting conditions.[25] Moreover, studies on the environmental impact of PLA disposal have shown that chemical, and, even more so, mechanical recycling are more sustainable End-of-Life alternatives to composting.[26] With the increasing necessity to rethink the current linear economy, End-of-Life scenarios for biobased polymers have become highly relevant. Distributed recycling via AM could give new life to waste polymers and make PLA a circular material.[27] The economic value of distributed recycling is significant, with several companies already exploring the transformation of postconsumer plastic into feedstocks for 3D printing.[28] However, there are very few examples in literature of thermo-mechanical recycling for blend biomaterials containing lignin.[29,30]

In the present work, we evaluated the compatibility of different types of lignins with PLA. Two technical lignins were isolated under different conditions: alkali kraft lignin (KL) and LignoBoost lignin (LB), and one additional Phenolated Organosolv lignin (POL). The latter was prepared using an in situ stabilization method (see SI), as an alternative to postmodified lignins due to its expected better compatibility with PLA, as indicated by the Hildebrand solubility parameters (see SI). This type of lignin can be obtained in one step directly from raw biomass under so-called active stabilization strategy, thereby avoiding additional modification steps.[31,32] Compatibility with PLA can be further improved through reactive extrusion, similar to the approach demonstrated by Mimini et al.[17] Filaments of PLA with high loadings of POL (up to 70 wt %) were produced by extrusion to determine the maximum limit for the use of this type of lignin as an additive in PLA. The filaments were tested for 3D printing, and their thermal and mechanical properties were evaluated. In the final part of this study, we focused on the thermo-mechanical recycling of PLA 30 wt % POL blends to include an outlook on the viability of reprocessing PLA blends, thereby aiming to reduce the environmental impact of 3D printing.

EXPERIMENTAL SECTION

Materials. Industrial PLA filament (Silver PLA filament) was purchased from Prusa Polymers a.s., Prague, Czech Republic, the number-average molecular weight was determined to be 84000 g/mol (Figures S15, S16, eqs S4 and S5); for properties see SI Table S5. Dialkali (kraft) lignin (KL) (#471003) was purchased from Merck. Modified Organosolv lignin (POL) was obtained from fractionation and modification of pine sawdust (see SI). LignoBoost UPM BioPiva 100 lignin (LB) was purchased from UPM Biochemicals (Helsinki, Finland).

Preparation of Filaments. The filaments utilized for FDM printing were extruded using a Filabot EX2 single screw extruder (Filabot Inc., Barre, VT) at a temperature of 180 °C. Prior to mixing and extrusion, pelletized industrial PLA filament and lignins were dried at 70 °C overnight to prevent hydrolysis of the PLA during the extrusion process.[16] Filaments were produced on a 15 g scale, apart from POL30-R0 (100 g scale) that was chosen for recycling experiments and multiple dog-bone specimens printing for analysis. After the first extrusion, the resulting filaments were pelletized and subjected to a second extrusion under identical conditions to improve miscibility between the components. The same procedure was followed for the fabrication of pure PLA filaments for fair comparison of the materials properties. The composition of the blend filaments is outlined in Table 1.

3D Printing. Type V dog-bone specimens (ASTM D638) were fabricated using a Prusa i3MK3S printer (Prusa, Prague, Czech Republic) equipped with a 0.4 mm diameter nozzle. The printing temperature was set to 215 °C, while the bed temperature was maintained at 60 °C. The specimens were printed with a layer height of 0.15 mm and a 15% infill density. To reinforce structural integrity, two solid layers, i.e., 100% infill, were printed at the top and bottom of the objects. The printing of the infill of the specimens was performed in two printing directions, i.e., horizontal and diagonal (see SI, Figure S1). Only diagonally printed dog-bone specimens are discussed in the article, and the horizontal data is given in SI.

Thermo-Mechanical Recycling. Mechanical recycling of the POL30 filament followed the established procedure for preparing PLA-lignin blends, as described previously. Initially, the twice-

https://doi.org/10.1021/acsapm.4c02208
ACS Appl. Polym. Mater. 2024, 6, 13574−13584

Table 1. Filaments Composition

sample name	type of lignin	lignin loading (wt %)	lignin content[a] (wt %)
POL30	phenolic OrganoSolv	30	40
POL30-R0	phenolic OrganoSolv	30	36
POL50	phenolic OrganoSolv	50	50
POL70	phenolic OrganoSolv	70	69
KL30	dialkaline (kraft lignin)	30	37
LB30	LignoBoost (kraft lignin)	30	30

[a]Lignin content in the filament in accordance with char content.

extruded filament (POL30-R0) was pelletized and then subjected to extrusion at 180 °C to yield the one-time recycled filament (R1). This process was repeated sequentially with each reprocessing cycle of the material labeled incrementally. After each cycle, the recycled filaments were employed for 3D printing. A schematic illustration outlining the thermo-mechanical recycling process is given in Figure 1.

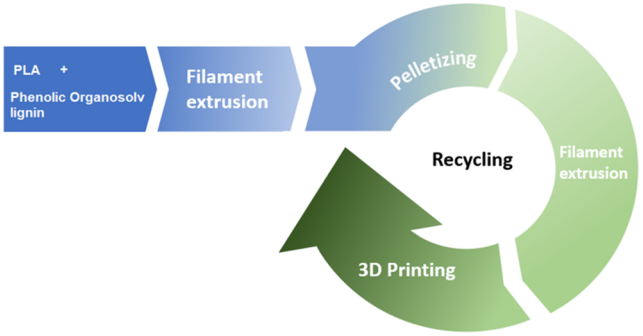

Figure 1. Thermo-mechanical recycling process for PLA and POL30 filaments.

Thermogravimetric Analysis (TGA). TGA was performed with a TGA/DSC 3+ (Mettler Toledo, Schwerzenbach, Switzerland). Samples with an approximate weight between 10 and 20 mg were heated from 25 to 700 °C under nitrogen flow in uncovered alumina crucibles at a rate of 10 K·min^{-1}. After the temperature reached 700 °C, the nitrogen flow was replaced by oxygen for the remainder of the experiment.

Differential Scanning Calorimetry (DSC). DSC measurements were performed in perforated aluminum crucibles on a DSC 3+ instrument (Mettler Toledo, Schwerzenbach, Switzerland). The samples were first cooled to −35 °C and then heated to 250 °C at a rate of 10 K·min^{-1}. Glass transition temperature, cold crystallization temperature, degree of crystallinity %, and melting temperature values were obtained from the second heating cycle.

The degree of crystallinity (χ %) was calculated by eq 1

$$\chi\ \% = \frac{\Delta H_m - \Delta H_{cc}}{\Delta H_m^{\circ}(1 - (\text{wt}\ \%/100))} \times 100 \quad (1)$$

where ΔH_m is the enthalpy of melting and ΔH_{cc} is the enthalpy of crystallization in the first heating run, ΔH°_m is the theoretical enthalpy of crystallization of the matrix if it was 100% crystalline, wt % is the mass percentage of PLA in the blend. The values used for ΔH°_m of PLA are 93 J·g^{-1}.[33]

Dynamic Mechanical Analysis (DMA). DMA tests were carried out using a DMA 850 (TA Instruments) with a heating rate of 3 °C·min^{-1} and a deformation frequency of 1 Hz. A strain of 0.05% was applied, along with a static force set at 1.2 times greater than the oscillating force. The temperature range for the measurements was from 0 to 160 °C. The measurements were conducted in triplicates. The sample filaments had diameters ranging from 1.2 to 1.8 mm and lengths between 15 and 20 mm. Pure lignin measurements were conducted using a powder sample holder under the following conditions: 30 mg of lignin, 1 Hz oscillations, 5 μm amplitude, 3 °C·min^{-1} heating rate, with the sample pocket clamped with a torque of 7 in.lb.[34]

Mechanical Testing. The maximum strength, elongation at break, and Young's modulus of the 3D−printed specimens were evaluated using a universal testing instrument (AGS-X, Shimadzu, Kyoto, Japan) equipped with a 5 kN load cell (the gauge length is 9.53 mm). The crosshead speed was set to 1 mm·min^{-1} for all tests. Each experiment was conducted in triplicate. The maximum stress point and elongation at break were determined. The slope of the curve in the elastic deformation region was used to calculate Young's modulus. Calculations were performed by considering 100% infill in the cross section, although 15% infill was used in all experiments. This will lead to an underestimation of the actual values. However, our aim was to compare the different materials, and this should not affect the comparison.

Nuclear Magnetic Resonance (NMR) Spectroscopy. All NMR spectra were recorded on a JEOL (400YH magnet) Resonance 400 MHz spectrometer. For ^{1}H, ^{13}C, and heteronuclear multiple bond correlation (HMBC) NMR spectra of blended filaments, chemical shifts δ are reported in ppm relative to solvent DMSO-d_6 (^{1}H: δ = 2.50; ^{13}C: δ = 39.52) and sample concentration was 13% (w/v). Coupling constants J are reported in Hz.

Determination of hydroxyl group content on POL, PLA, recycled polymer, and recycled polymer-POL lignin blends was carried out via quantitative ^{31}P NMR spectroscopy, based on previously published protocol.[17,35] Samples were fully dissolved in 0.5 mL of a solvent mixture of chloroform-*d* and pyridine (1:1.6 v/v, respectively) and internal standard solution consisting of internal standard (IS) endo-*N*-hydroxy-5-norbornene-2,3-dicarboximide (NHND, 3 mg·mL^{-1}) and relaxation agent chromium(III) acetylacetonate (5 mg·mL^{-1}). After sonication for 24 h, the phosphorylating agent 2-chloro-4,4,5,5-tetramethyl-1,2,3-dioxaphospholane (TMDP, 0.1 mL) was added. Samples were analyzed within 24 h after the addition of the phosphorylating agent. ^{31}P NMR spectra were recorded using 128 scans and a relaxation delay of 10 s. Data were processed in MestReNova software through which automatic baseline correction and phase correction were applied. Hydroxyl group content was determined by the integration of the following regions: NHND (151.5−152.1 ppm), aliphatic OH (146.0−146.6; 146.6−149.0), condensed OH (142.6−144.3 ppm), guaiacyl OH (139.0−140.0 ppm), *p*-hydroxyphenyl OH (137.0−138.5 ppm), and carboxylic acid OH (134.6−135.5 ppm). The integral values were then converted to millimolar OH groups per gram of lignin using eq 2, where R is the integration ratio of the region of interest over the internal standard region.

$$\text{mmol OH/g lignin} = \frac{R \times \text{NHND in NMR sample (mmol)}}{\text{dry weight of sample (g)}} \quad (2)$$

For all samples, the lignin content was calculated based on char values at 550 °C, vide infra.

RESULTS AND DISCUSSION

Characterization of PLA-Lignin 30 wt %. A minimum addition of 30 wt % was selected to assess the compatibility of the three different types of lignin with PLA. Notably, filaments produced from PLA blends with POL and LB exhibited uniform circular cross sections and precise diameter tolerances (SI, Figures S11 and S12). Conversely, KL failed to produce solid filaments due to its low melt viscosity.[10] The primary difference between LB and POL, on one side, and KL, on the other, which may contribute to PLA hydrolysis, is the presence of alkali residues in KL from the pulping process. The alkaline environment generated by KL likely causes hydrolysis of the PLA polymer, leading to a lower melt viscosity of the material blend.[36] This finding aligns well with the observed differences

https://doi.org/10.1021/acsapm.4c02208
ACS Appl. Polym. Mater. 2024, 6, 13574−13584

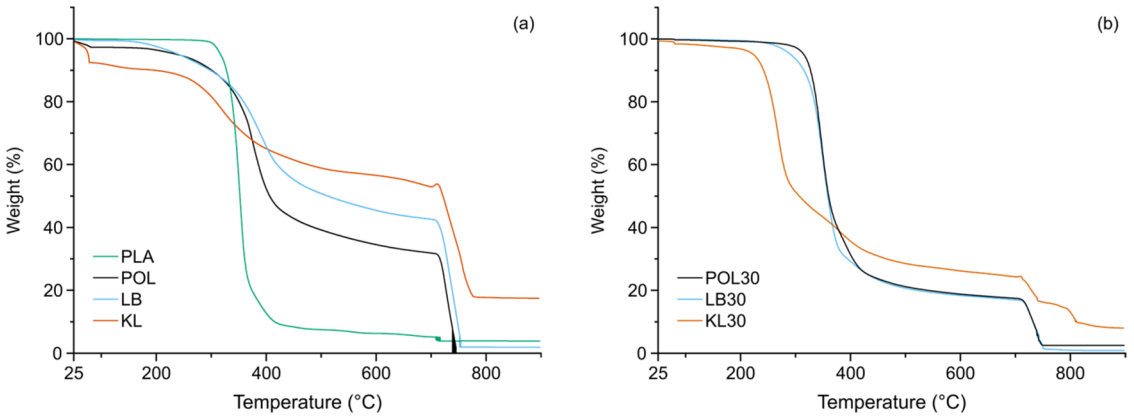

Figure 2. TGA thermogram: (a) pure starting materials and (b) filament blends of PLA-lignin. Data are presented as the mean of triplicate experiments.

Table 2. Thermal Properties of Pure Materials and Blends (Filaments)

blend	$T_{d,onset}$ (°C)	$T_{d,max}$ (°C)	$Char_{550\ °C}$ (%)	$Char_{calcd}$[a] (%)	T_g (°C)	T_{cc} (°C)	T_m (°C)	X (%)
PLA	318	352	6.9		59	119	150	0[b]
POL	328	380	33.8		134	NA		
KL	252	318	49.6		NA	NA		
LB	308	395	47.8		150			
POL30	322	347	19.8	15.0	59	117	150	0[b]
							161	
POL30-R0	337	353	16.6	15.0	59	119	151	0[b]
LB30	317	351	19.3	19.3	59		153	
KL30	246	269	25.8	19.7	59[b]	88[b]	167[b]	
POL50	294	340	20.2	20.0	59	112	152	1[b]
							168	
POL70	266	349	24.9	25.2	58	110	147	19[b]
							157	
							173	

[a]Recalculated on wt % fractions of char pure materials ω PLA char + ω lignin char, char content was calculated for weight loss % between 100 and 550 °C. [b]Value from the first heating cycle. TGA data are presented as the mean of triplicate experiments (for standard deviation (SD) values see Table S6).

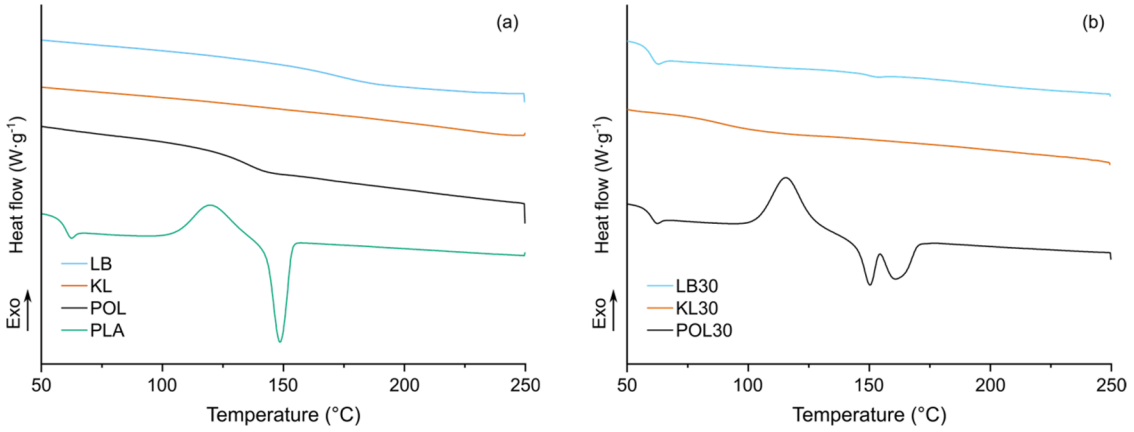

Figure 3. DSC second heating cycles of pure compounds (a) and filaments of PLA-lignin blends (b). Data are presented as the mean of triplicate experiments.

in filament quality and provides insight into the underlying mechanisms influencing compatibility between PLA and various lignin types when the lignin content exceeds 5%.[12]

The thermogravimetric analysis (TGA, Figure 2) and first derivative thermogravimetric (DTG, Figure S2) curves were obtained under a nitrogen atmosphere for the extruded filaments of pure materials and 30 wt % PLA-lignin blends. The initial degradation temperature ($T_{d,onset}$), the maximum degradation temperature ($T_{d,max}$), and char residue at 550 °C for both pure materials and blends are reported in Table 2. As expected, the structural complexity of lignin results in a broader range of decomposition temperatures.[15,17] Compared to the PLA filament, LB and KL degradation initiates at lower temperatures, while POL exhibits a 10 °C higher $T_{d,onset}$. The

https://doi.org/10.1021/acsapm.4c02208
ACS Appl. Polym. Mater. 2024, 6, 13574−13584

maximum weight loss for all pure compounds occurs between 300 and 400 °C, with LignoBoost (LB) exhibiting the highest $T_{d,max}$ at 395 °C. Char residue at 550 °C for POL, KL, and LB was found to be 33, 58, and 48%, respectively. The decrease in $T_{d,onset}$ in the KL blend can be ascribed to the degradation of low molecular weight compounds present in lignin, which is consistent with observations in the pure polymer.[37] Peak degradation is not significantly affected in blends of POL or LB relative to the pure PLA, however, the inclusion of KL exerts a catalytic effect on polymer thermal degradation, lowering $T_{d,max}$ by 100 °C relative to PLA. Additionally, char residue in the blends is increased compared to PLA, owing to the highly aromatic structure of lignin and its ability to form char.[7] While for LB30 the reduction of mass at 550 °C is in accordance with the 30 wt % loading percentage, the mass loss for POL30 and KL30 samples is lower at this temperature than expected ($Char_{calcd}$, Table 2). We attribute the difference to the loss of PLA during compounding, caused by the extruder design, which resulted in a higher loading of lignin than expected (40% for POL30 and 36% for KL30).

Glass transition temperature (T_g), melting temperature, and Cold Crystallization temperature (T_{cc}) were derived from the second heating cycle of DSC, as shown in Table 2 and Figure 3. In the case of KL, T_g could not be detected during the second heating scan as a consequence of the degradation process of KL that occurred during the first heating cycle. In the first heating cycle, a broad peak appears at 104 °C (Figure S3a, previously reported as T_g for KL[21]), by comparison with TGA (Figure 2a) and this peak can be attributed to loss of moisture from the sample. Similarly, for the one-time extruded filament, irreversible melting of the material occurred during the first heating cycle (Figure S3b), preventing the observation of a distinct T_g in the second heating cycle (Figure 3b).

While POL and LB possess higher T_g, no increase in the glass transition temperature was observed for the respective blend filaments. In the case of POL30, a reduction in T_{cc} and the presence of double melting peaks were observed. The multiple melting behavior is ascribed to the melting of the α'- and the α-crystals developed during the DCS heating cycle (Figure 3b).[38,39] PLA in the POL30 blend material can crystallize, but the rate of crystallization is very slow, at least under extrusion conditions. The degree of crystallinity (χ %) in the blend material is 0% (POL30, Table 2). In contrast, the blend containing LignoBoost lignin (LB30) exhibited no cold crystallization and a very small melting peak, indicating that this type of lignin hinders PLA crystallization (Figure 3b).

Next, the printability and mechanical properties of the different blend materials were evaluated. Both 30 wt % blends of POL and LB were successfully used to print dog-bone-shaped specimens (Figure S4). Although the inclusion of lignin did not lead to enhancements in PLA mechanical properties, a comparison between the two lignin blends revealed better mechanical properties, for POL30. Specifically, the modulus of elasticity, tensile strength, and elongation at break for POL blends exceeded those of LB lignin blends in both printing orientations (Figures 4, S10, and Table S4). Most likely, the lower molecular weight POL allows it to act more effectively as a plasticizer compared to LB, with molecular weights of 4600 and 5000 g mol^{-1}, respectively (Table S3). Additionally, the introduction of phenol groups and the lower concentration of total hydroxy groups in the modified lignin (5.33 mmol g^{-1} for POL and 6.58 mmol g^{-1} for LB) are expected to bring the Hildebrand solubility parameters of lignin and PLA closer together, resulting in better compatibility between POL and PLA compared with the PLA-LB blend.

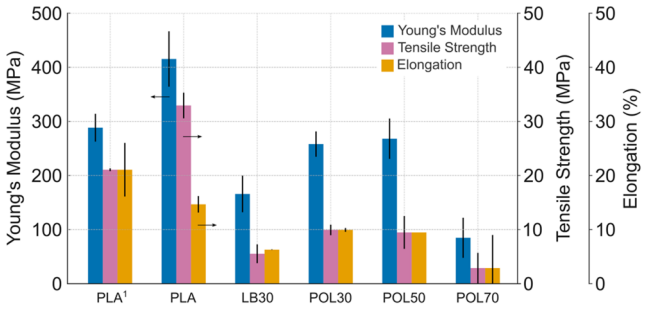

Figure 4. Mechanical properties of 3D−printed dog-bone specimens of PLA, LB30, and different POL wt % loadings; PLA^1-3D−printed dog-bone specimens from commercial ready PLA filament. Data are presented as the mean ± SD of triplicate experiments.

Characterization of PLA−POL at Higher wt % Additions. In the second part of our investigation, we explored the maximum permissible amount of lignin that can be used as a PLA additive. To the best of our knowledge, this study represents the first instance of producing PLA filaments containing more than 40% lignin (Table S1).

Based on the results of thermal and mechanical tests, POL lignin emerged as the most promising lignin type for further investigation. Filaments containing 50 and 70 wt % POL were successfully extruded at 180 °C, displaying perfectly circular cross sections and tight diameter tolerances. These filaments, alongside POL30, were utilized for 3D printing of dog-bone shapes, and their thermal and mechanical properties were evaluated. However, the printability was significantly influenced by the lignin content in the filament. Higher amounts of lignin (70 wt %) resulted in rougher surfaces and poor melt flow, primarily due to the presence of small lignin clusters within the PLA structure. Layer adhesion was also impaired, leading to defects in the dog-bone specimens (Figure S5). While compounding PLA with more than 50 wt % phenolic organosolv lignin is feasible (Figure S6), it is not ideal for filament production for 3D printing. To address the challenges associated with such high PLA dilution with lignin, further compatibilization should be considered to improve interfacial interactions within the blend.[40]

While degradation initiates at lower temperatures in POL50 and POL70, $T_{d,max}$ exhibits no significant change. Additionally, an increase in the char residue at 550 °C was also observed (Table 2 and Figure 5a). The char residue values obtained for the blend filaments align with the calculated char percentages based on values obtained for pure components, assuming an additive effect (eqs S1 and S2). The ability of lignin to produce char proves advantageous when seeking halogen-free flame retardant properties in materials.[7]

DSC analysis of 50 and 70 wt % PLA−POL blends revealed double and triple melting peaks, respectively (Figure 5b). As in the case of POL30, the presence of multiple melting peaks can indicate the occurrence of melting/recrystallization/melting processes with or without changes in crystal structure.[41,42] Cold crystallization temperature (T_{cc}) and enthalpy of crystallization decrease with increasing lignin content in the blend. The degree of crystallinity, as calculated from DSC results, was 0% for the PLA sample. The addition of 30 and 50% POL did not significantly affect the crystallinity, remaining at 0 and 1% respectively. However, a higher POL

https://doi.org/10.1021/acsapm.4c02208
ACS Appl. Polym. Mater. 2024, 6, 13574−13584

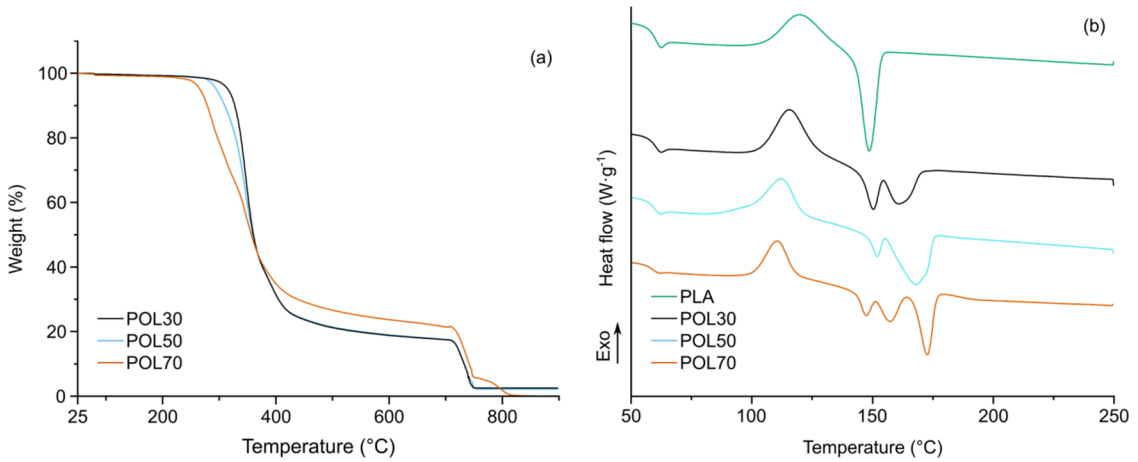

Figure 5. PLA−POL blend filaments with varying lignin loadings (a) TGA; (b) DSC second heating cycle. Data are presented as the mean of triplicate experiments.

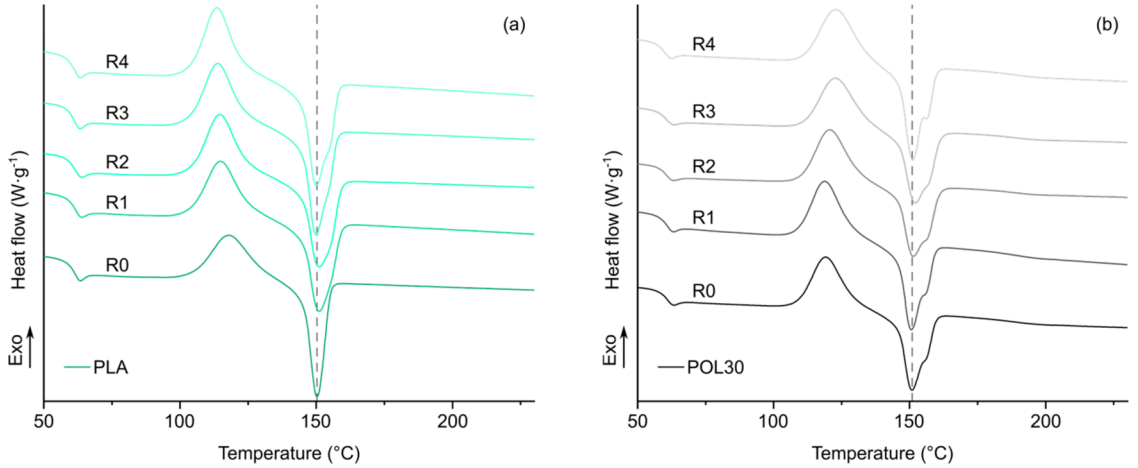

Figure 6. DSC curves of successively recycled filament materials: (a) recycled PLA and (b) recycled POL30. Data are presented as the mean of triplicate experiments.

content, 70 wt %, increased the crystallinity to 19%. Materials containing up to 50% POL are essentially amorphous.

The mechanical properties of dog-bone specimens of PLA−POL blends are displayed in Figure 4. POL50 exhibited mechanical properties comparable to POL30, while elasticity and tensile strength decreased at the highest loading of 70 wt %. The reduction in tensile strength can be attributed to the inherently lower tensile strength of lignin compared to neat PLA. Consequently, even if the components of the blend are highly compatible, a reduction in the overall tensile strength is still expected. Moreover, increasing the lignin content can lead to lignin agglomeration, further contributing to the deterioration of the mechanical properties. Notably, Young's modulus for POL30 and POL50 aligns very well with the direct printing of commercial PLA filament. The blend filaments were also found to be more brittle than the pure PLA, with elongation (%) significantly reduced by the addition of lignin. The deterioration of mechanical properties in blends containing more than 5 wt % lignin is in agreement with previous studies.[17] A tensile strength drop was reported by Gordobil et al. already at lignin concentrations of 10 wt %, at 20 wt % concentration the tensile strength decrease was reported to be 54%.[15,33] Similarly, Obielodan and Alshammari studies on PLA-Organosolv reported a tensile strength decrease for blend material in comparison with PLA of 68 and 50% respectively for 10 and 20 wt % of lignin in the blends.[16,43] Our blends exhibited a similar deterioration of tensile strength but at a higher lignin concentration, making phenolic Organosolv lignin a good candidate when high lignin concentrations (>40 wt %) in PLA are desired. Since the mechanical tests were conducted on 3D−printed specimens, the quality and directionality of the printing is a relevant factor in the assessment of blend mechanical properties. Diagonal-printed specimens demonstrated a more promising mechanical profile compared with their horizontally printed counterparts (Figure S10). Layer adhesion during printing also proved to be a significant factor in determining the mechanical properties. At higher lignin loadings, poor layer adhesion resulted in easily peeling layers, making printing difficult and significantly impacting the tensile test results (Figure S5). The POL30 filament was further benchmarked by printing the 3DBenchy[44] model in half scale (the boat, SI Figure S7). This challenging print is typically designed to evaluate the performance of 3D printers but can also be utilized to assess filament printability. While there is room for improvement, an overall acceptable level of print quality was achieved with the POL30 filament, demonstrating good layer adhesion and acceptable surface smoothness.

https://doi.org/10.1021/acsapm.4c02208
ACS Appl. Polym. Mater. 2024, 6, 13574−13584

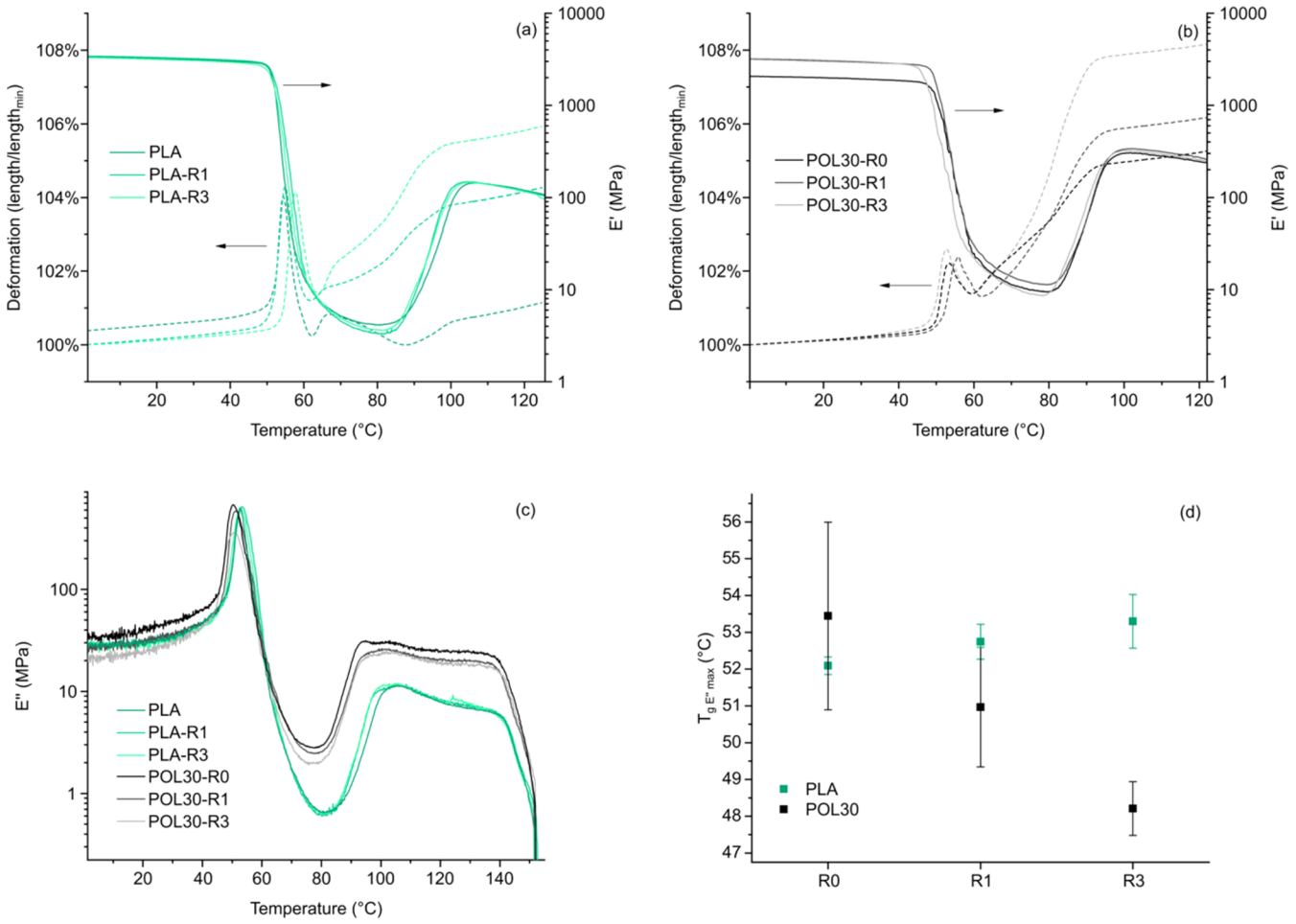

Figure 7. DMA characterization of recycled PLA and PLA-lignin blends (filaments): (a) extension and storage modulus (E') for PLA; (b) PLA-lignin blends; (c)loss modulus (E''); and (d) glass transition temperature determined as the maximum of the E'' peak.

Recycling. Recycling studies were conducted to evaluate the impact of mechanical recycling on the thermal characteristics of the POL30-R0 blend and, consequently, the feasibility of reusing the material for 3D printing. The reprocessed blend filament was compared to the reprocessed industrial PLA filament to ascertain the influence of lignin on PLA degradation following successive mechanical recycling cycles. The PLA−POL filament underwent reprocessing until it failed to produce 3D-printed dog-bone specimens. We observed that the blend filament could indeed be effectively utilized for 3D printing across three recycling cycles.

The DSC analysis of the recycled PLA filaments revealed an increase in the crystallinity and a gradual decrease in T_{cc} (Figure 6a). This phenomenon, as reported by previous literature on PLA recycling, may signify polymer degradation and formation of imperfect crystals during mechanical recycling.[25] Additionally, the presence of a second crystalline phase in the material was evidenced by the broadening of the melting peak and the emergence of a shoulder in the last reprocessing cycle. In the blend filament, T_{cc} shifted to higher temperatures after each recycling (Figure 6b). Reprocessed PLA filaments exhibited lower viscosity,[28] potentially promoting higher homogeneity between PLA and lignin. However, the presence of lignin could impair the crystallization of thermally degraded PLA. A shoulder indicative of a second melting peak was also visible for the blend filament, although the melting temperature remained unaffected by reprocessing.

The typical DMA profile for PLA can be seen in Figure 7: a glass transition region between 50 and 70 °C followed by cold crystallization at 120 °C and a melting point at around 150 °C.[45] The successive recycling steps of the pure PLA did not change any of the onsets of these events, nor did it significantly change the storage (E') or loss (E'') modulus as the glassy or rubbery plateau (Table 3). The standard deviation (SD) of the T_g was small, whereas the SD of the moduli values were large. The broad range in moduli values between replicates is likely due to the filaments being somewhat twisted and not completely straight. No significant difference was found in modulus values between recycling steps, similarly to a previous publication on recycled PLA.[46]

Table 3. Storage Modulus (E') and Glass Transition Temperature with Standard Deviations

sample	E' at 25 °C (MPa)	E' at 110 °C (MPa)	T_g E'' max (°C)
PLA	3280 ± 100	137 ± 8	52.7 ± 0.4
PLA-R1	3280 ± 130	133 ± 11	53.7 ± 0.3
PLA-R3	3330 ± 290	140 ± 8	54.3 ± 1.0
POL30-R0	2510 ± 350	256 ± 42	54.8 ± 2.7
POL30-R1	2070 ± 150	284 ± 8	52.0 ± 1.4
POL30-R3	2990 ± 330	317 ± 17	49.7 ± 0.6
POL			185 ± 3

https://doi.org/10.1021/acsapm.4c02208
ACS Appl. Polym. Mater. 2024, 6, 13574−13584

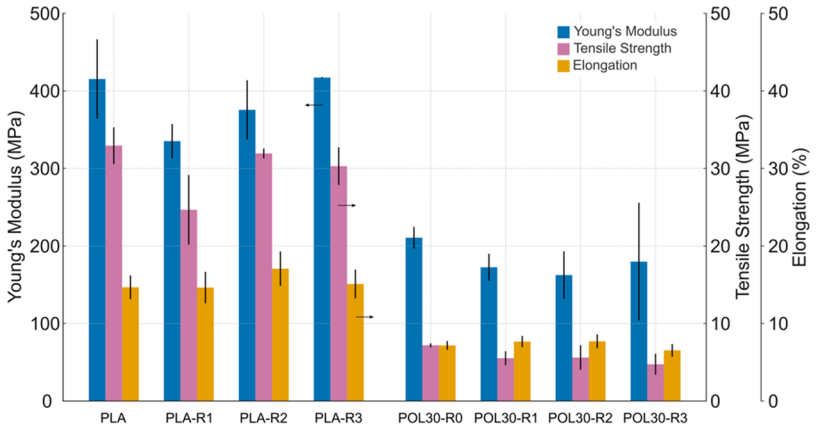

Figure 8. Mechanical properties of 3D−printed dog-bone specimens of recycled PLA and POL30-R0. Data are presented as the mean ± SD of triplicate experiments.

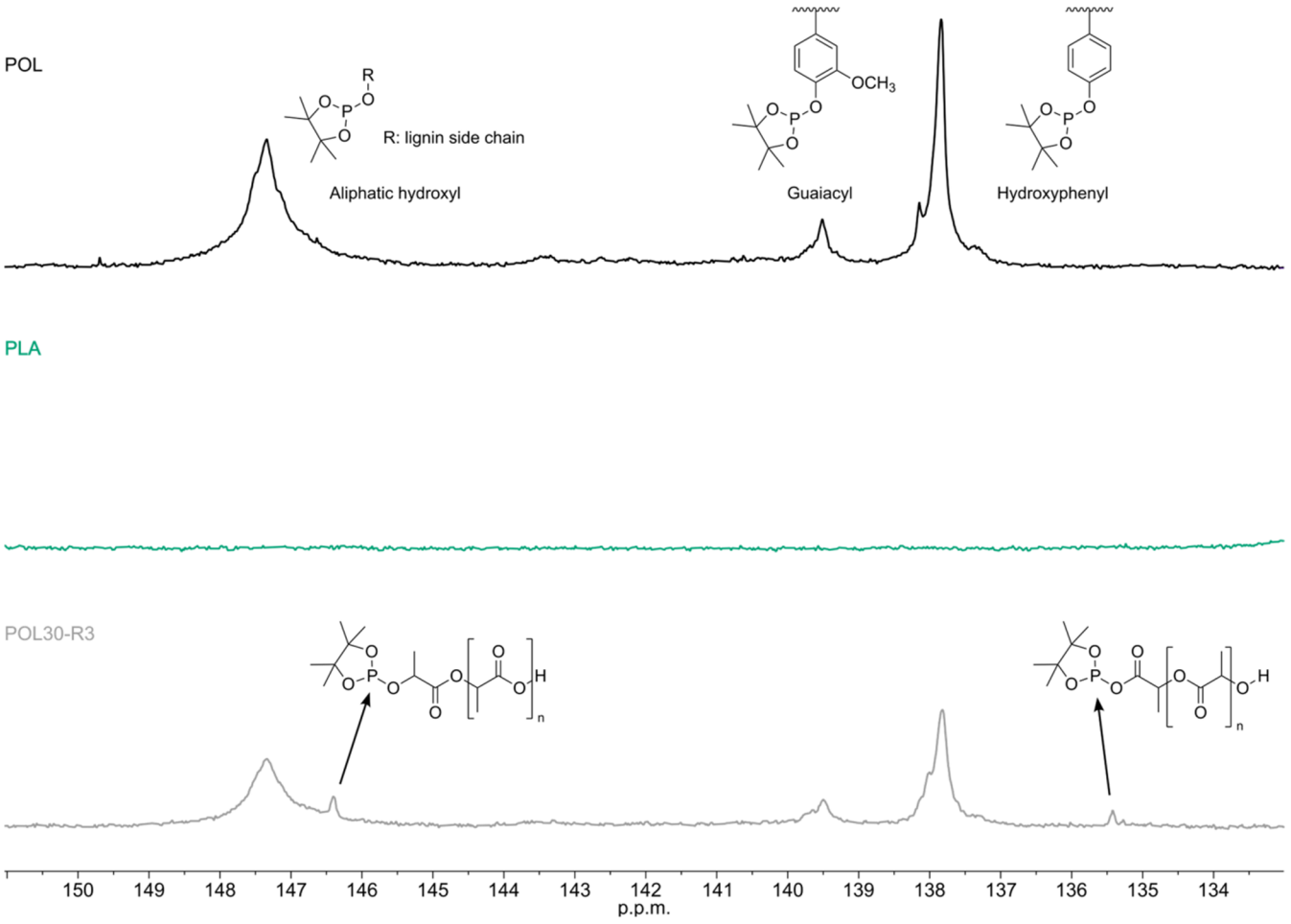

Figure 9. ^{31}P NMR spectra of POL, PLA, and POL30-R3.

Upon addition of the lignin, the DMA curves change (Figure 7b). The E' of the glassy plateau drops, most likely due to weak points introduced by the additive. At the rubbery plateau (around 110 °C), E' increases (Table 3), presumably as the lignin is still a glass, which adds strength to the rubbery matrix. The T_g value remains statistically unchanged.

With recycling of the PLA-lignin blend, the E' and E'' values increase, both in the glassy and rubbery state (lignin is a glass still at 110 °C, see Figure S8). It is apparent that increasing recycling leads to a more homogeneous material with smaller lignin particles, resulting in better cohesion and thus increased moduli values.

The T_g of the PLA-lignin blend also decreases with increasing recycling cycles (Figure 7d). This subtle decrease was not seen with DSC, likely due to its lower sensitivity as compared to DMA. The reason for this is most likely chain scission (as discussed further in the Nuclear Magnetic Resonance (NMR) Spectroscopy section). Another explanation could be a change in the confinement of the polymer matrix. Additives with poor interactions with the polymer

https://doi.org/10.1021/acsapm.4c02208
ACS Appl. Polym. Mater. 2024, 6, 13574−13584

matrix can reduce the T_g of the material, as the interface gives the polymers more room for movement, i.e., they are less confined than in the bulk.[47] Thus, if the contact surfaces between PLA and lignin increase with repeated recycling, the amount of PLA with greater degrees of freedom would increase, consequently resulting in a lower overall T_g. For instance, the opposite effect, an increased T_g due to restricted movement of PLA at the particle interphase, was seen for blends with talc.[48]

As the DMA instrument records the length of the sample, it is possible to monitor the shrinkage and extension of the material; however, as the static force changes throughout the experiment, these results are not as informative as an unchanging static force would be. Upon the glass transition, the materials are seen to extend and then suddenly contract. This behavior has been observed for PLA samples processed through extrusion[49] and can be explained by thermal shrinkage, i.e., recoiling of stretched-out polymer chains upon the glass transition. The decreasing shrinkage upon further recycling seen in both sets of samples suggests that the orientation is reduced. The high temperature of the recycling most likely leads to chain scission, and the shorter chains are less susceptible to orientation and recoiling effects.

The mechanical and printability properties of PLA appear unaffected by recycling; although swelling of the filament was observed after consecutive reprocessing, the material properties remained unchanged throughout the recycling study, as confirmed by DMA results (Figure 8). The PLA−POL blend filament exhibited a decrease in tensile strength and Young's modulus by 20% after the second recycling. The addition of lignin might aggravate PLA weakening, thereby lowering its strength and elasticity after reprocessing. One possible explanation is that, after multiple recycling cycles, lignin is more dispersed in the PLA matrix. This dispersion can weaken the polymer by increasing the spacing between PLA chains. On the other hand, this can result in a more ductile material and improved elongation (+8%). A more homogeneous material can also be the result of polymer thermal degradation: the shorter PLA chains resulting from thermal degradation may lead to increased diffusion of lignin within the matrix.

Qualitative and quantitative hydroxyl group content in the recycled blends was monitored via ^{31}P NMR spectroscopy and HMBC (Figure 9 and Table S3). Figure 9 shows the ^{31}P NMR spectra of phenolic organosolv lignin, recycled PLA, and recycled POL30-R0. While no signals from PLA are visible in the ^{31}P spectrum of PLA-R3, distinct signals are observable in the ^{31}P spectra of POL30-R3 and lignin. The comparison of the spectra reveals the appearance of two additional signals at δ 146.4 ppm (aliphatic OH) and δ 135.4 ppm (carboxylic acid OH) in the recycled blend filament. These signals can be attributed to PLA terminal hydroxyl and carboxylic groups, in agreement with previously reported ^{31}P NMR data on phosphitylated PLA.[50] From a comparison between the OH content (eq S3, Table S3, Figures S13 and S14) in lignin and in POL30, a decrease in lignin's aliphatic and phenolic OH appear evident in the blend filament. Concomitantly, the amount of carboxylic OH is only 10% the amount of aliphatic OH from PLA. The lower amount of free carboxylic groups versus aliphatic groups in PLA and the reduction of aliphatic and phenolic lignins could be an indication of PLA carboxylic groups reacting with lignin hydroxy groups during filament reprocessing. A further indication of PLA−POL bond formation is provided by the HMBC spectrum (Figure S9), where a correlation appears between the PLA's methine proton (δ 5.2 ppm) and a carbon atom (δ 161.9 ppm) attributed to a phenolic quaternary carbon in phenolic lignin. While PLA degrades during recycling cycles, lignin seems to be unaffected by the thermal treatment as no significant change could be detected in the amount of condensed OH and guaiacyl OH groups after each recycling step.

CONCLUSIONS

In this work, we produced and systematically characterized poly(lactic acid)-lignin blends using two different unmodified technical kraft lignins and phenolated organosolv lignin (POL), which was produced in situ during the pulping process. Compared to the technical lignins used in this study, blends with 30 wt % POL and PLA exhibited good printability and improved mechanical properties. Additionally, blends with 50 wt % POL demonstrated similar properties to those of 30% POL, with both materials remaining amorphous under extrusion conditions. High lignin content blends, with up to 70 wt % POL, were also produced and utilized in FDM 3D printing to create dog-bone-shaped specimens. Furthermore, blend formulations with up to 30 wt % phenolated organosolv lignin showed good recyclability over three consecutive reprocessing cycles, which included grinding, reextrusion, and printing. Reusing and recycling plastics such as PLA provide several significant benefits, including reducing plastic waste, conserving resources, lowering greenhouse gas emissions, and overall supporting sustainability efforts. With several effective commercialized methods for recycling PLA already available, it is crucial that any modifications to PLA not compromise its recyclability. Enhancing PLA with new properties should go hand in hand with preserving or even improving its recyclability to fully realize these environmental and economic benefits. This approach supports a circular economy where plastics are effectively reused and recycled, minimizing waste and conserving valuable resources. Our results demonstrate that phenolated organosolv lignin shows promise as a sustainable candidate for PLA-lignin blends, aligning with these goals.

ASSOCIATED CONTENT

Supporting Information

The Supporting Information is available free of charge at https://pubs.acs.org/doi/10.1021/acsapm.4c02208.

Additional experimental details of phenolated organosolv lignin preparation procedure, PLA properties, calculation of Hildebrand parameters for lignins, additional information on SEC, TGA, DSC, DMA, photos of specimens, NMR spectra, and ^{31}P NMR data (PDF)

AUTHOR INFORMATION

Corresponding Authors

Maxim V. Galkin − *Nanotechnology and Functional Materials, Department of Materials Science and Engineering, Ångström Laboratory, Uppsala University, SE-751 03 Uppsala, Sweden;* orcid.org/0000-0001-6543-7674; Email: maxim.galkin@angstrom.uu.se

Johan Gising − *Nanotechnology and Functional Materials, Department of Materials Science and Engineering, Ångström Laboratory, Uppsala University, SE-751 03 Uppsala, Sweden;* orcid.org/0000-0001-8852-6071; Email: johan.gising@angstrom.uu.se

Authors

Serena Frasca − *Nanotechnology and Functional Materials, Department of Materials Science and Engineering, Ångström Laboratory, Uppsala University, SE-751 03 Uppsala, Sweden;* orcid.org/0009-0006-1938-8123

Christos S. Katsiotis − *Nanotechnology and Functional Materials, Department of Materials Science and Engineering, Ångström Laboratory, Uppsala University, SE-751 03 Uppsala, Sweden;* orcid.org/0000-0002-0154-3627

Åke Henrik-Klemens − *Applied Chemistry, Chemistry and Chemical Engineering, Chalmers University of Technology, SE-412 96 Gothenburg, Sweden; FibRe—Centre for Lignocellulose-Based Thermoplastics, Department of Chemistry and Chemical Engineering, Chalmers University of Technology, SE-412 96 Gothenburg, Sweden;* orcid.org/0009-0007-1976-3285

Anette Larsson − *Applied Chemistry, Chemistry and Chemical Engineering, Chalmers University of Technology, SE-412 96 Gothenburg, Sweden; FibRe—Centre for Lignocellulose-Based Thermoplastics, Department of Chemistry and Chemical Engineering and Wallenberg Wood Science Center, Chalmers University of Technology, SE-412 96 Gothenburg, Sweden;* orcid.org/0000-0002-6119-8423

Maria Strømme − *Nanotechnology and Functional Materials, Department of Materials Science and Engineering, Ångström Laboratory, Uppsala University, SE-751 03 Uppsala, Sweden;* orcid.org/0000-0002-5496-9664

Jonas Lindh − *Nanotechnology and Functional Materials, Department of Materials Science and Engineering, Ångström Laboratory, Uppsala University, SE-751 03 Uppsala, Sweden;* orcid.org/0000-0001-5196-4115

Complete contact information is available at: https://pubs.acs.org/10.1021/acsapm.4c02208

Author Contributions

The manuscript was written through the contributions of all authors, who have given approval to the final version of the manuscript. S.F. performed most of the work, including materials preparation, 3D printing, characterization, data acquisition, and wrote the initial draft. C.K. and M.G. performed proof-of-concept experiments. Å.H.K. conducted DMA analysis, co-wrote, and proofread the manuscript. A.L., J.L., and M.S. secured funding and proofread the manuscript. A.L., M.G., and J.G. contributed by supervising the research work, guiding the experiments and analyses, and proofreading and edited the manuscript.

Funding

The authors gratefully acknowledge financial support from the Swedish Research Council for Sustainable Development (Formas, Grant no: 2022-02042). Å.H.K. and A.L. acknowledge support by Fiber—a Vinnova-funded Competence Centre for Design for Circularity: Lignocellulose-based Thermoplastics (2019-00047).

Notes

The authors declare the following competing financial interest(s): GM, JL, and JG are inventors on a Swedish Patent Application (2350558-9) that covers the preparation and isolation of functionalized lignins via a phenols-assisted process. The patent application is owned by AB Karl Hedin Bio Innovation. JL, MS, MG, and JG are partially involved in AB Karl Hedin Bio Innovation activities.

ACKNOWLEDGMENTS

The authors would like to acknowledge AB Karl Hedin Sågverk for providing pine sawdust.

REFERENCES

(1) Ji, A.; Zhang, S.; Bhagia, S.; Yoo, C. G.; Ragauskas, A. J. 3D Printing of Biomass-Derived Composites: Application and Characterization Approaches. *RSC Adv.* **2020**, *10*, 21698−21723.

(2) Andanje, M. N.; Mwangi, J. W.; Mose, B. R.; Carrara, S. Biocompatible and Biodegradable 3D Printing from Bioplastics: A Review. *Polymers* **2023**, *15* (10), 2355.

(3) Gupta, B.; Revagade, N.; Hilborn, J. Poly(Lactic Acid) Fiber: An Overview. *Prog. Polym. Sci.* **2007**, *32*, 455−482.

(4) Wojtyła, S.; Klama, P.; Baran, T. Is 3D Printing Safe? Analysis of the Thermal Treatment of Thermoplastics: ABS, PLA, PET, and Nylon. *J. Occup. Environ. Hyg.* **2017**, *14* (6), D80−D85.

(5) Elsawy, M. A.; Kim, K. H.; Park, J. W.; Deep, A. Hydrolytic Degradation of Polylactic Acid (PLA) and Its Composites. *Renewable Sustainable Energy Rev.* **2017**, *79*, 1346−1352, DOI: 10.1016/j.rser.2017.05.143.

(6) Zhou, S. J.; Wang, H. M.; Xiong, S. J.; Sun, J. M.; Wang, Y. Y.; Yu, S.; Sun, Z.; Wen, J. L.; Yuan, T. Q. Technical Lignin Valorization in Biodegradable Polyester-Based Plastics (BPPs). *ACS Sustainable Chem. Eng.* **2021**, *9*, 12017−12042.

(7) Zhang, R.; Xiao, X.; Tai, Q.; Huang, H.; Hu, Y. Modification of Lignin and Its Application as Char Agent in Intumescent Flame-Retardant Poly(Lactic Acid). *Polym. Eng. Sci.* **2012**, *52* (12), 2620−2626.

(8) Kim, Y.; Suhr, J.; Seo, H.-W.; Sun, H.; Kim, S.; Park, I.-K.; Kim, S.-H.; Lee, Y.; Kim, K.-J.; Nam, J.-D. All Biomass and UV Protective Composite Composed of Compatibilized Lignin and Poly (Lactic-Acid). *Sci. Rep.* **2017**, *7*, No. 43596.

(9) Zhuang, Z.; Li, T.; Ning, Z.; Jiang, N.; Gan, Z. Melt and nucleation reinforcement for stereocomplex crystallites in poly(L-lactide)/lignin-grafted-poly(D-lactide) blend. *Eur. Polym. J.* **2022**, *167*, No. 111072.

(10) Yao, J.; Odelius, K.; Hakkarainen, M. Microwave Hydrophobized Lignin with Antioxidant Activity for Fused Filament Fabrication. *ACS Appl. Polym. Mater.* **2021**, *3* (7), 3538−3548.

(11) Mearaj, S.; Ajaz, A. M.; Kim, T. M.; Choi, J. W.; Kim, M.; Choi, J. W. Bioactive and Hemocompatible PLA/Lignin Bio-Composites: Assessment of In Vitro Antioxidant Activity for Biomedical Applications. *ACS Appl. Bio Mater.* **2023**, *6* (9), 3648−3660.

(12) Bužarovska, A.; Blazevska-Gilev, J.; Pérez-Martnez, B. T.; Balahura, L. R.; Pircalabioru, G. G.; Dinescu, S.; Costache, M. Poly(L-Lactic Acid)/Alkali Lignin Composites: Properties, Biocompatibility, Cytotoxicity and Antimicrobial Behavior. *J. Mater. Sci.* **2021**, *56* (24), 13785−13800.

(13) Cicala, G.; Latteri, A.; Saccullo, G.; Recca, G.; Sciortino, L.; Lebioda, S.; Saake, B. Investigation on Structure and Thermomechanical Processing of Biobased Polymer Blends. *J. Polym. Environ.* **2017**, *25* (3), 750−758.

(14) Park, C.-W.; Youe, W.-J.; Kim, S.-J.; Han, S.-Y.; Park, J.-S.; Lee, E.-A.; Kwon, G.-J.; Kim, Y.-S.; Kim, N.-H.; Lee, S.-H. Effect of Lignin Plasticization on Physico-Mechanical Properties of Lignin/Poly-(Lactic Acid) Composites. *Polymers* **2019**, *11*, 2089.

(15) Gordobil, O.; Delucis, R.; Egüés, I.; Labidi, J. Kraft Lignin as Filler in PLA to Improve Ductility and Thermal Properties. *Ind. Crops Prod.* **2015**, *72*, 46−53.

(16) Alshammari, S.; Ameli, A. Polylactic Acid Biocomposites with High Loadings of Melt-Flowable Organosolv Lignin. *Int. J. Biol. Macromol.* **2023**, *242*, No. 125094.

(17) Mimini, V.; Sykacek, E.; Nurul Ain Syed Hashim, S.; Holzweber, J.; Hettegger, H.; Fackler, K.; Potthast, A.; Mundigler, N.; Rosenau, T. Compatibility of Kraft Lignin, Organosolv Lignin and Lignosulfonate With PLA in 3D Printing. *J. Wood Chem. Technol.* **2019**, *39* (1), 14−30.

(18) Tanase-Opedal, M.; Espinosa, E.; Rodríguez, A.; Chinga-Carrasco, G. Lignin: A Biopolymer from Forestry Biomass for Biocomposites and 3D Printing. *Materials* **2019**, *12* (18), No. 3006.
(19) Dai, L.; Liua, R.; Si, C. A novel functional lignin-based filler for pyrolysis and feedstock recycling of poly(l-lactide). *Green Chem.* **2018**, *20*, 1777−1783.
(20) Liu, R.; Dai, L.; Hu, L.-Q.; Zhou, W.-Q.; Si, C.-L. Fabrication of high-performance poly(l-lactic acid)/lignin-graft-poly(d-lactic acid) stereocomplex films. *Mater. Sci. Eng., C* **2017**, *80*, 397−403.
(21) Esakkimuthu, E. S.; DeVallance, D.; Pylypchuk, I.; Moreno, A.; Sipponen, M. H. Multifunctional Lignin-Poly (Lactic Acid) Biocomposites for Packaging Applications. *Front. Bioeng. Biotechnol.* **2022**, *10*, No. 1025076.
(22) Maldhure, A. V.; Ekhe, J. D.; Deenadayalan, E. Mechanical Properties of Polypropylene Blended with Esterified and Alkylated Lignin. *J. Appl. Polym. Sci.* **2012**, *125*, 1701−1712.
(23) Makri, S. P.; Xanthopoulou, E.; Valera, M. A.; Mangas, A.; Marra, G.; Ruiz, V.; Koltsakidis, S.; Tzetzis, D.; Zoikis Karathanasis, A.; Deligkiozi, I.; Nikolaidis, N.; Bikiaris, D.; Terzopoulou, Z. Poly(Lactic Acid) Composites with Lignin and Nanolignin Synthesized by In Situ Reactive Processing. *Polymers* **2023**, *15* (10), 2386.
(24) Rahman, M. A.; Santis, D. De.; Spagnoli, G.; Ramorino, G.; Penco, M.; Phuong, V. T.; Lazzeri, A. Biocomposites Based on Lignin and Plasticized Poly(L-Lactic Acid). *J. Appl. Polym. Sci.* **2013**, *129*, 202−214.
(25) Pérez-Fonseca, A. A.; González-López, M. E.; Robledo-Ortíz, J. R. Reprocessing and Recycling of Poly(Lactic Acid): A Review. *J. Polym. Environ.* **2023**, *31* (10), 4143−4159.
(26) Cosate de Andrade, M. F.; Souza, P. M. S.; Cavalett, O.; Morales, A. R. Life Cycle Assessment of Poly(Lactic Acid) (PLA): Comparison Between Chemical Recycling, Mechanical Recycling and Composting. *J. Polym. Environ.* **2016**, *24* (4), 372−384.
(27) Al Rashid, A.; Koç, M. Additive Manufacturing for Sustainability and Circular Economy: Needs, Challenges, and Opportunities for 3D Printing of Recycled Polymeric Waste. *Mater. Today Sustain.* **2023**, *24*, No. 100529.
(28) Cruz Sanchez, F. A.; Boudaoud, H.; Hoppe, S.; Camargo, M. Polymer Recycling in an Open-Source Additive Manufacturing Context: Mechanical Issues. *Addit. Manuf.* **2017**, *17*, 87−105.
(29) Åkesson, D.; Fazelinejad, S.; Skrifvars, V. V.; Skrifvars, M. Mechanical Recycling of Polylactic Acid Composites Reinforced with Wood Fibres by Multiple Extrusion and Hydrothermal Ageing. *J. Reinf. Plast. Compos.* **2016**, *35* (16), 1248−1259.
(30) Avella, A.; Ruda, M.; Gioia, C.; Sessini, V.; Roulin, T.; Carrick, C.; Verendel, J.; Lo Re, G. Lignin Valorization in Thermoplastic Biomaterials: From Reactive Melt Processing to Recyclable and Biodegradable Packaging. *Chem. Eng. J.* **2023**, *463*, No. 142245.
(31) Renders, T.; Van Den Bosch, S.; Koelewijn, S.-F.; Schutyser, W.; Sels, B. F. Lignin-First Biomass Fractionation: The Advent of Active Stabilisation Strategies. *Energy Environ. Sci.* **2017**, *10*, 1551.
(32) Galkin, M. From Stabilization Strategies to Tailor-Made Lignin Macromolecules and Oligomers for Materials. *Curr. Opin. Green Sustainable Chem.* **2021**, *28*, No. 100438.
(33) Gordobil, O.; Egüés, I.; Llano-Ponte, R.; Labidi, J. Physicochemical Properties of PLA Lignin Blends. *Polym. Degrad. Stab.* **2014**, *108*, 330−338.
(34) Henrik-Klemens, Å.; Caputo, F.; Ghaffari, R.; Westman, G.; Edlund, U.; Olsson, L.; Larsson, A. The Glass Transition Temperature of Isolated Native, Residual, and Technical Lignin. *Holzforschung* **2024**, *78* (4), 216−230.
(35) Meng, X.; Crestini, C.; Ben, H.; Hao, N.; Pu, Y.; Ragauskas, A. J.; Argyropoulos, D. S. Determination of Hydroxyl Groups in Biorefinery Resources via Quantitative 31P NMR Spectroscopy. *Nat. Protoc.* **2019**, *14* (9), 2627−2647.
(36) Jung, J. H.; Ree, M.; Kim, H. Acid- and Base-Catalyzed Hydrolyses of Aliphatic Polycarbonates and Polyesters. *Catal. Today* **2006**, *115* (1−4), 283−287.
(37) Yan, Q.; Zhang, H.; Ketelboeter, T.; Peng, Y.; Wan, C.; Cai, Z. Tuning Thermal and Graphitization Behaviors of Lignin via Complexation with Transition Metal Ions for the Synthesis of Multilayer Graphene-Based Materials. *RSC Adv.* **2024**, *14* (11), 7592−7600.
(38) Pantani, R.; De Santis, F.; Sorrentino, A.; De Maio, F.; Titomanlio, G. Crystallization Kinetics of Virgin and Processed Poly(Lactic Acid). *Polym. Degrad. Stab.* **2010**, *95* (7), 1148−1159.
(39) Mu, C.; Xue, L.; Zhu, J.; Jiang, M.; Zhou, Z. Mechanical and Thermal Properties of Toughened Poly(L-Lactic) Acid and Lignin Blends. *Bioresources* **2014**, *9* (3), 5557−5566.
(40) Ou, W. X.; Weng, Y.; Zeng, J. B.; Li, Y. D. Fully Biobased Poly(Lactic Acid)/Lignin Composites Compatibilized by Epoxidized Natural Rubber. *Int. J. Biol. Macromol.* **2023**, *236*, No. 123960.
(41) Yasuniwa, M.; Iura, K.; Dan, Y. Melting Behavior of Poly(l-Lactic Acid): Effects of Crystallization Temperature and Time. *Polymer* **2007**, *48* (18), 5398−5407.
(42) Lee, K. H.; Lo, C. T. Additives for Enhancing the Crystallizability and Degradability of Electrospun Poly(l-Lactide) Fibers. *ACS Appl. Polym. Mater.* **2023**, *5* (11), 9525−9535.
(43) Obielodan, J.; Vergenz, K.; Aqil, D.; Wu, J.; Ellistrem, L. M. In *Characterization of PLA/Lignin Biocomposites for 3D Printing*, Solid Freeform Fabrication 2019: Proceedings of the 30th Annual International Solid Freeform Fabrication Symposium—An Additive Manufacturing Conference, SFF 2019, University of Texas at Austin, 2019; pp 998−1007.
(44) Creative Tools. The Jolly 3D Printing Torture-Test Website, 2024. https://www.3dbenchy.com/dimensions/.
(45) Cristea, M.; Ionita, D.; Iftime, M. M. Dynamic Mechanical Analysis Investigations of Pla-Based Renewable Materials: How Are They Useful? *Materials* **2020**, *13* (22), 5302.
(46) Patti, A.; Acierno, S.; Cicala, G.; Zarrelli, M.; Acierno, D. Assessment of Recycled PLA-Based Filament for 3D Printing. *Mater. Proc.* **2021**, *7* (1), No. 16.
(47) Napolitano, S.; Glynos, E.; Tito, N. B. Glass Transition of Polymers in Bulk, Confined Geometries, and near Interfaces. *Rep. Prog. Phys.* **2017**, *80* (3), No. 036602.
(48) Shakoor, A.; Thomas, N. L. Talc as a Nucleating Agent and Reinforcing Filler in Poly(Lactic Acid) Composites. *Polym. Eng. Sci.* **2014**, *54* (1), 64−70.
(49) Sikorska, W.; Zięba, M.; Musioł, M.; Kowalczuk, M.; Janeczek, H.; Chaber, P.; Masiuchok, O.; Demchenko, V.; Talanyuk, V.; Iurzhenko, M.; Puskas, J. E.; Adamus, G.; Paton Electric, E. O. Forensic Engineering of Advanced Polymeric Materials-Part VII: Degradation of Biopolymer Welded Joints. *Polymers* **2020**, *12*, 1167.
(50) Hirata, M.; Kobayashi, K.; Kimura, Y. Synthesis and Properties of High-Molecular-Weight Stereo Di-Block Polulactides with Non-equivalent D/L Ratios. *J. Polym. Sci., Part A: Polym. Chem.* **2010**, *48* (4), 794−801.

https://doi.org/10.1021/acsapm.4c02208
ACS Appl. Polym. Mater. 2024, 6, 13574−13584